Journal of Medicinal Chemistry

Subscriber access provided by UNIV OF NEBRASKA - LINCOLN

Article

Monothiocarbamates strongly inhibit carbonic anhydrases in vitro and possess intraocular pressure lowering activity in an animal model of glaucoma

Daniela Vullo, Mariaconcetta Durante, Francesco Saverio Di Leva, Sandro Cosconati, Emanuela Masini, Andrea Scozzafava, Ettore Novellino, Claudiu T Supuran, and Fabrizio Carta

J. Med. Chem., **Just Accepted Manuscript** • DOI: 10.1021/acs.jmedchem.6b00462 • Publication Date (Web): 02 Jun 2016

Downloaded from http://pubs.acs.org on June 7, 2016

Just Accepted

"Just Accepted" manuscripts have been peer-reviewed and accepted for publication. They are posted online prior to technical editing, formatting for publication and author proofing. The American Chemical Society provides "Just Accepted" as a free service to the research community to expedite the dissemination of scientific material as soon as possible after acceptance. "Just Accepted" manuscripts appear in full in PDF format accompanied by an HTML abstract. "Just Accepted" manuscripts have been fully peer reviewed, but should not be considered the official version of record. They are accessible to all readers and citable by the Digital Object Identifier (DOI®). "Just Accepted" is an optional service offered to authors. Therefore, the "Just Accepted" Web site may not include all articles that will be published in the journal. After a manuscript is technically edited and formatted, it will be removed from the "Just Accepted" Web site and published as an ASAP article. Note that technical editing may introduce minor changes to the manuscript text and/or graphics which could affect content, and all legal disclaimers and ethical guidelines that apply to the journal pertain. ACS cannot be held responsible for errors or consequences arising from the use of information contained in these "Just Accepted" manuscripts.

ACS Publications

Journal of Medicinal Chemistry is published by the American Chemical Society. 1155 Sixteenth Street N.W., Washington, DC 20036

Published by American Chemical Society. Copyright © American Chemical Society. However, no copyright claim is made to original U.S. Government works, or works produced by employees of any Commonwealth realm Crown government in the course of their duties.

Monothiocarbamates strongly inhibit carbonic anhydrases in vitro and possess intraocular pressure lowering activity in an animal model of glaucoma

Daniela Vullo,[1] Mariaconcetta Durante,[2] Francesco Saverio Di Leva,[3] Sandro Cosconati,[4] Emanuela Masini,[2] Andrea Scozzafava,[1] Ettore Novellino,[3] Claudiu T. Supuran[1,5*] and Fabrizio Carta,[1*]

[1] Università degli Studi di Firenze, Polo Scientifico, Laboratorio di Chimica Bioinorganica, Rm. 188, Via della Lastruccia 3, 50019 Sesto Fiorentino (Florence), Italy.

[2] Università degli Studi di Firenze, Dipartimento NEUROFARBA, Sezione di Farmacologia, Viale Pieraccini 6, 50139 Florence, Italy.

[3] Department of Pharmacy, University of Naples "Federico II", Via D. Montesano 49, 80131 Naples, Italy.

[4] DiSTABiF, Seconda Università di Napoli, Via Vivaldi 43, 81100 Caserta, Italy.

[5] Università degli Studi di Firenze, NEUROFARBA Dept., Sezione di Scienze Farmaceutiche, Via Ugo Schiff 6, 50019 Sesto Fiorentino (Florence), Italy.

Keywords: Monothiocarbamates (MTCs), carbonic anhydrase inhibitors (CAIs), metalloenzymes, glaucoma.

Abstract: A series of monothiocarbamates (MTCs) were prepared from primary/secondary amines and COS, as potential carbonic anhydrase (CA, EC 4.2.1.1) inhibitors, using the dithiocarbamates, the xanthates and the trithiocarbonates as lead compounds. The MTCs effectively inhibited the pharmacologically relevant human (h) hCAs isoforms I, II, IX and XII *in vitro*, and showed K_Is spanning between the low and medium nanomolar range. By means of a computational study the MTC moiety binding mode on the CAs was explained. Furthermore, a selection of MTCs were evaluated in a normotensive glaucoma rabbit model for their intraocular pressure (IOP) lowering effects, and showed interesting activity.

Introduction.

The metalloenzyme Carbonic Anhydrases (CAs, EC 4.2.1.1) are widely expressed within all living organisms and are genetically encoded by six unrelated families indicated with the Greek letters α−, β−, γ−, δ−, ζ− and η−CAs.[1-3] Among the various reactions catalyzed by the CAs, the reversible hydration of carbon dioxide to afford bicarbonate and protons, represents the unique one with physiological consequences.[1c,d]

Such a simple reaction is deeply connected to fundamental biological processes, which include respiration, electrolyte secretions, pH homeostasis, bone resorption, biosynthesis of lipids, nucleic acids and glucose. [1-13] Thus the modulation of such an equilibrium through the CAs catalytic activities, definitely represents a powerful approach for the treatment of various diseases.[4-13] To date, the use of small molecules CA activators (CAAs) as anticonvulsant/antiepileptic appear quite promising. Even better, CAAs were demonstrated to be efficient for the treatment of central nervous system (CNS) affecting diseases such as Alzheimer's.[4-7]Conversely the use of CA inhibitors (CAIs) is more common, since their introduction in the 60's as antihypertensive and antiglaucoma agents. [8-10] Nowadays CAIs are employed for the treatment of a vast array of diseases, including epilepsy, metabolic related pathologies (e.g., obesity), as well as for the management or diagnosis of hypoxic tumors. [1-16] Pharmacological therapies based on the use of CA modulators (i.e., inhibitors/activators), mainly take advantage of the essential role played by the carbon dioxide catalyzed reactions within the cells life cycles. In addition, the variety of CAs expressed within organisms is strictly dependent from their physio/pathological conditions. Thus since all isozymes differ for their kinetic properties as well as for cellular, sub-cellular and tissue distributions it is clear that a successful CA modulation approach therapy resides on its ability to properly address such a biochemical diversity .[1c,12]

Such a scenario clearly introduces to the main problem to be faced within the CAs field, which is represented by the search of selective modulators targeting the preferred isoforms. [11a, 12]

The application of the tail approach to the classical zinc binding CAIs, such as the sulfonamides and their bioisosters, represented the preferred medicinal chemistry approach to address the isoform selectivity issues. [3d,12b,17] In addition, the many efforts conducted towards the identification of new chemical classes acting as CAIs, drove to the discovery of the coumarins [18a,b] and their congeners, [18c-h] the phenols [19] and the polyamines. [20] All of them were demonstrated to possess different inhibition mechanisms by means of kinetics as well as X-ray crystallographic experiments in adduct with various hCA isoforms.[17-20]

In particular *in vitro* screening of inorganic anions allowed to identify the trithiocarbonate (CS_3^-) as a low micromolar (μM) inhibitor of the highly abundant cytosolic hCAs (I, II) and of the tumor associated isoform IX. [21] The CS_3^- enzymatic zinc-binding ability was disclosed through its crystallographic adduct with hCA II. [22] The pioneering work on the CS_3^- ion as CAI, triggered the investigation towards small molecules containing the zinc-binding dithio-moiety, such as the dithiocarbamates [23] the xanthates [24] and the thioxanthates or trithiocarbonates. [24] All these classes showed excellent inhibition potencies against the α- as well as the pathogenous β-CAs with K_Is spanning in the low-medium nanomolar (nM) range.

Herein, as an extension of our studies we report for the first time the synthesis, characterization as well as *in vitro* kinetic profiling against the hCAs I, II, IX and XII of the monothiocarbamates (MTCs). A plausible enzymatic binding mode is also proposed by means of molecular modeling studies. A selection of such compounds was evaluated in a normotensive glaucoma rabbit model for the possible effect as IOP lowering agents.

Results and Discussion.

Compounds Design and Synthesis.

The drug design rationale of this project is based on the replacement of the sulphur atom of the DTCs moiety with an oxygen instead (Figure **1A**). As reported below the synthetic methodology consisted of a direct carbamoylation between primary/secondary amines with carbonyl monosulfide (COS) in the presence of sodium hydroxide as a base (Figure **1B**).

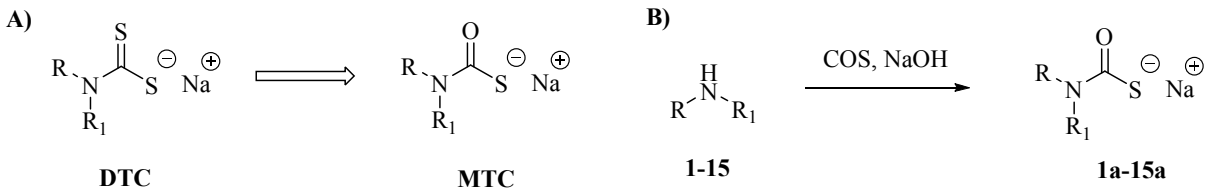

Figure 1A) Rational design of the MTCs; **B**) General synthetic procedure for MTCs **1a-15a**

The selected amines contained alkyl/aralkyl moieties allowing us to obtain a series of 15 MTC derivatives as sodium salts (**Table 1**). All compounds were characterized by means of ^{1}H, ^{13}C NMR spectroscopy and HRMS and were >98 % pure, as determined by HPLC (see the Experimental Section for details). The insertion of the mothiocarbamate moiety was confirmed by ^{13}C NMR, which gave the characteristic signal at 180-186 ppm using dmso-d_6 as solvent.

CA Inhibition.

All compounds synthesized, **1a-15a**, were tested *in vitro* for their inhibitory properties against the physiological relevant hCA isoforms I, II, IX and XII, by means of the stopped-flow carbon dioxide hydration assay.[25] Their activities were compared to the standard CAI acetazolamide (**AAZ**) as well their structurally related moieties (i.e. the Dithiocarbamate **16**, Xanthate **17)** and to the inorganic CS_3^{2-} ion (Table 1).

Table 1. hCA I, II, IX, and XII inhibition data with MTCs **1a−15a**, Dithiocarbamate **16**, Xanthate **17** and Trithiocarbonate by a Stopped-Flow CO_2 Hydrase Assay.[25]

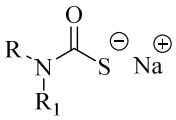

1a-15a

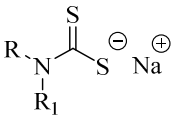

16

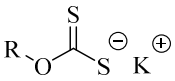

17

No.			K_I (nM)[a]			
	R	R_1	hCA I	hCA II	hCA IX[b]	hCA XII
1a	H	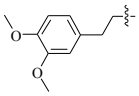	891	26.7	15.2	3.3
2a	H	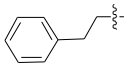	>2000	43.7	21.5	4.7
3a	H	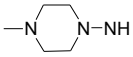	>2000	35.0	7.7	9.2
4a	*n*-Pr	*n*-Pr	>2000	46.7	12.5	7.9
5a	*n*-Bu	*n*-Bu	909	>2000	6.8	7.5
6a	*i*-Bu	*i*-Bu	681	43.0	9.2	3.4
7a	Et	*n*-Bu	700	>2000	6.2	7.2
8a	Me		827	44.5	22.1	1.9
9a	Me	Bn	>2000	>2000	11.7	44.5

10a			569	>2000	13.5	2.8
11a			876	22.4	10.4	6.8
12a	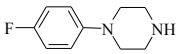		895	46.8	6.5	3.8
13a	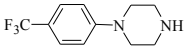		>2000	43.6	11.8	7.5
14a	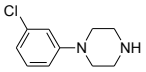		686	>2000	4.9	23.0
15a	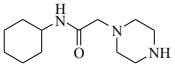		949	45.9	14.0	7.3
16[c]	H	Bn	4.1	0.70	19.2	11.5
17[d]	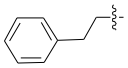		64.1	5.4	58.0	63.3
CS_3^{2-}			8.7 (μM)[e]	8.8 (μM)[e]	9.7 (μM)[f]	120 (μM)[f]
AAZ			250	12	25	5.7

[a] Means from three different assays. Errors were within ±5−10% of the reported values (data not shown). [b] Catalytic domain. [c] From ref. 23c. [d] From ref. 24. [e] From ref. 21a. [f] From ref. 21b.

The data reported above clearly showed the MTCs **1a-15a** act as high-medium potency CAIs against the abundantly expressed isoforms I and II, with K_I values spanning between 0.95-0.57 μM and 46.8-22.4 nM respectively. On the other hand, the inhibition constants against the tumor

associated isoforms IX and XII were comprised in the low nM range and comparable with the standard sulfonamide **AAZ** (K_I 5.7 nM). Overall the MTCs showed to be more potent CAIs when compared to the CS_3^{2-} ion (K_Is in the μM range), and definitely more selective in inhibiting the tumor associated isoforms (hCA IX and XII) over the cytosolic ones (I, II) when compared to the Dithiocarbamate **16** and Xanthate **17**. Such compounds were considered as comparison since their binding modes with hCAs were all similar (see later in the text).

The following Structure-Activity Relationships (SAR) are reported:

i) The hCA I is the less inhibited isoform from the MTCs herein reported. Our investigation started with the insertion of the MTC moiety into primary amines such as the 2,4-dimethoxy phenylethylamine, which showed a high nM inhibition value (compound **1a** K_I 891 nM). The removal of the methoxy substituents or the use of the 4-methyl-piperazin-1-ylamine as primary amine instead resulted in a complete loss (K_I>2000) of the inhibition activity (compound **2a** and **3a** respectively). Insertion of the MTC moiety into secondary amines bearing linear or branched alkyl chains, such as in compounds **5a-8a**, resulted in K_Is values between 681-909 nM, with the only exception of **4a** and **9a** which were ineffective (K_Is >2000 nM). Interestingly merging of the smallest alkyl substituent into a heterocyclic moiety, such as in the morpholine**10a**, resulted in a slight increase of the inhibition potency against the hCA I (K_I 569 nM), which was the highest within the series. Surprisingly, the replacement of the morpholine oxygen in **10a** with a nitrogen and insertion of two MTC functionalities to afford compound **11a**, caused a 1.5 fold decrease in the inhibition potency (K_I 876 nM). Substitution of a piperazinic proton in **11a** with the *p*-fluorophenyl moiety, as in **12a**, did not sensibly affect the inhibition potency (K_I 895 nM). However the introduction of the *p*-trifluoromethyl instead, as in compound **13a**, suppressed the inhibition activity (K_I>2000) which was restored with the *m*-chlorophenyl moiety (compound **14a** K_I 686 nM). Exploitation of the piperazine scaffold was also accomplished by introducing the MTC moiety into the antiulcer drug Hexaprazole to give the derivative **15a** (K_I of 949 nM).

ii) Interesting inhibition data were obtained for the highly abundanthCA II isoform which is of particular interest for the pharmacological treatment of glaucoma. The MTCs **1a-3a**, showed good affinity data with K_I values comprised between 26.7 and 43.7 nM. Opposite to the hCA I, the removal of the methoxy substituents in **1a** to afford **2a** resulted only in a 1.63 fold enhancement of the K_I (26.7 and 43.7 nM respectively). Among the substituted secondary amines bearing the MTC moiety only the symmetrical *n*-propyl **4a**, *i*-propyl **6a** and the asymmetric **8a** derivatives resulted good inhibitors of the hCA II (K_Is 46.7, 43.0 and 44.5 nM respectively), whereas the remaining ones were ineffective (K_Is >2000). Interestingly the MTC morpholine**10a** showed no inhibition against the hCA II (K_I>2000), whilst the disubstituted piperazine **11a** is a rather effective CAI with a K_I of 22.4 nM, which makes it the most potent hCA II inhibitor within the series. Interestingly the piperazine monosubstituted MTCs containing the fluoro-aryl moieties, such as **13a** and **12a**, or an α-amidoalkyl chain, as for the Hexaprazole **15a**, showed K_Is spanning between 43.6-45.9 nM and comparable with those of **4a**, **6a** and **8a**. Switch of the fluorine to chlorine and change of its position from *para* to *meta*, as in compound **14a**, resulted in loss of the inhibition potency (K_I>2000).

iii) All the synthesized MTCs showed excellent affinities against the tumor associated hCA IX with K_I values comprised between 6.2 and 22.1 nM, and thus comparable to the standard **AAZ** (K_I 25 nM). Again, removal of the methoxy substituents such as in **1a** to afford **2a** resulted in a lowering of their inhibition potencies (K_Is of 15.2 and 21.5 nM, respectively). Conversely, the hydrazino-methyl piperazine MTC **3a** resulted highly potent CAI (K_I 7.7 nM). Secondary amine MTC derivatives **4a-11a** were all good hCA IX inhibitors with K_Is spanning between 6.2 and 22.1 nM. Interestingly the introduction into the piperazine scaffold of the *para*-fluorophenyl moiety, as in compound **12a**, resulted in a strengthening of the inhibition activity (K_I 6.5 nM), which conversely showed a 1.81 and 2.15 fold K_I increase when the trifluoromethyl and the alfa-amidoalkyl moiety were inserted instead (compounds **13a** and **15a** respectively). Noteworthy the *meta*-chorophenyl derivative **14a** reported a sensible increase of the potency with a K_I of 4.9 nM, which is the most active in inhibiting the hCA IX among all the MTCs tested.

iv) The second transmembrane hCA isoform (hCA XII) was also strongly inhibited by all synthesized compounds. In particular MTCs **1a-3a**, obtained from primary amines, were low nanomolar inhibitors (K_Is 3.3, 4.7, 9.2 nM respectively) and comparable to the standard CAI sulfonamide **AAZ** (K_I 5.7 nM). The secondary symmetrical MTC containing amines, such as **4a** and **5a,** showed similar inhibition potencies (K_Is 7.9 and 7.5 nM respectively). Interestingly the substitution of the of the linear *n*-butyl chains in **5a** with the branched isomers, as in compound **6a**, resulted in a 2.2 fold increase of the inhibition potency (K_I 3.4 nM). De-symmetrization of the open alkyl moieties, compounds **7a** and **9a**, resulted in a sensible increase of the K_Is to 7.2 and 44.3 nM respectively, with the only exception represented from the compound **8a** which showed the highest inhibition potency against the hCA XII (K_I 1.9 nM). The MTCs bearing the secondary cyclic scaffolds, such as the morpholine**10a** and the piperazine**11a**, also resulted quite efficient inhibitors of the hCA XII showing K_Is of 2.8 and 6.8 nM. Among the various substituents inserted into the piperazine scaffold, the *para*-fluorophenyl containing MTC **12a** was the most potent with a K_I of 3.8 nM, while its trifluoromethyl derivative **13a** resulted 2 folds less potent (K_I 7.5 nM) and comparable to the Hexaprazole MTC **15a** (K_I 7.3 nM). The *meta*-chlorophenyl**14a** was the less effective hCA XII inhibitor of the piperazine series having a K_I of 23 nM.

Thus, in general, all the synthesized compounds showed interesting inhibition properties against the physiological relevant hCAs. Whilst the hCA I was poorly inhibited, the catalytically more efficient hCA II showed a better profile with the bis substituted piperazine derivative **11a**as the most potent within the series (K_I 22.4 nM). The tumor associated hCA isoforms hCA IX and XII were strongly inhibited from the MTCs herein reported with K_I values in the low nanomolar range and by far lower to the standard CAI **AAZ**. In particular the piperazine derivative **14a** showed a K_I of 4.9 nM against the hCA IX and the asymmetric MTC **8a** a K_I of 1.9 nM against the hCA XII.

Molecular Modeling.

To elucidate the binding mode of our MTCs at the α-CA active site, molecular docking studies were performed on compound **2a**, which was demonstrated to have good inhibitory properties against hCAs II, IX and XII (**Table 1**). Docking of **2a** into the X-ray crystal structure of hCA II (PDB code 3P5L) predicts that the ligand binds deep into the enzyme catalytic site in its anionic form, with its MTC moiety chelating the Zn^{2+} ion in a monodentate manner. In this regards, calculations suggest that the metal ion can be alternatively coordinated through the sulfur or the oxygen atom. However, previous spectroscopic and crystallographic studies indicated that MTC derivatives coordinate metal ions through sulfur, since the negative charge distribution resulted mainly shifted towards this atom.[26] Thus the lowest energy docking pose among those showing the sulfur-Zn^{2+} coordination was considered for our investigations (**Figure 2a**). In this pose, the MTC oxygen atom in compound **2a** interacts through a hydrogen bond with the T200 residue, and in analogy with many zinc-binding CAIs.[7] The phenylethyl moiety extends from the enzymatic cavity towards the hydrophobic region of the CA binding pocket, establishing a T-shaped stacking interaction with F131, and favorable van der Waals contacts with F131, V135, L141, L198 and P202. Noteworthy this binding pose resulted highly superimposable with a DTC inhibitor in complex with hCA II of comparable potency and early reported by some of us (see **Figure S1** in Supporting Information).[23a]

Additional docking calculations were also attained for compounds **4a, 11a** and **12a** (see **Figure S2** in Supporting Information). These ligands were chosen because of their different steric demands in the interaction with the enzyme counterpart thereby allowing to rationalize the different hCA II inhibitory potencies of our MTCs. Dockings of the latter compounds would in fact suggest that: *i*) in the case of *N*-alkyl di-substituted MTCs (**4a-7a**), long linear chains may not be hosted in the enzyme cavity for steric reasons, explaining why compounds featuring a *n*-butyl chain (**5a** and **7a**) are inactive towards the hCA II enzyme; *ii*) more hydrophilic compounds (**8a**, **10a, 11a** and **15a**) may compensate the loss of lipophilic contacts by establishing an additional hydrogen bond with the Q92 side chain (see **Figure S2b**). This interaction is not established by the morpholine ring of **10a** (data not shown), which is indeed inactive towards hCAII; *iii*) for aromatic substituted

derivatives (**1a**, **2a**, **9a**, and **12a-14a**), a short chain linking the ring and the MTC moiety or *meta* substitutions on the terminal aryl ring should hamper the interactions with the residues lining the hydrophobic pocket (i.e. F131), thereby explaining the inactivity of compounds **9a** and **14a**.

Docking calculations also helped to elucidate the molecular bases for the slight selectivity profile of our MTC derivatives towards the tumor associated hCA IX and XII. Multiple sequence alignment of hCAs I, II, IX and XII showed that single point mutations occur at the binding cavities of these enzymes (see **Figure S3** in Supporting Information). Specifically, the bulky F131 residue in hCA II resulted replaced by the smaller valine (F131V) and alanine (F131A) in hCA IX and XII respectively. Interestingly, docking of compound **2a** into hCA IX and hCA XII (Figures **2b** and **2c**) reveals that these substitutions, although causing the loss of the highly stabilizing T-shaped π–π interaction, allow the ligand to penetrate deeper into the hydrophobic region of the active site, thus enhancing the contribution of desolvation to the overall ligand binding free energy. Finally, in hCA I the N67 and T200 amino acids are both replaced by a histidine residue, which might affect ligand binding for steric reasons. Moreover, the T200H substitution results in the loss of the key hydrogen bond established by the ligand MTC moiety in hCA II, IX and XII (Figure **3**). This would explain the inactivity of compound **2a**, and more generally the lower activity of our MTCs, against the hCA I compared to the other three isoforms considered in this study.

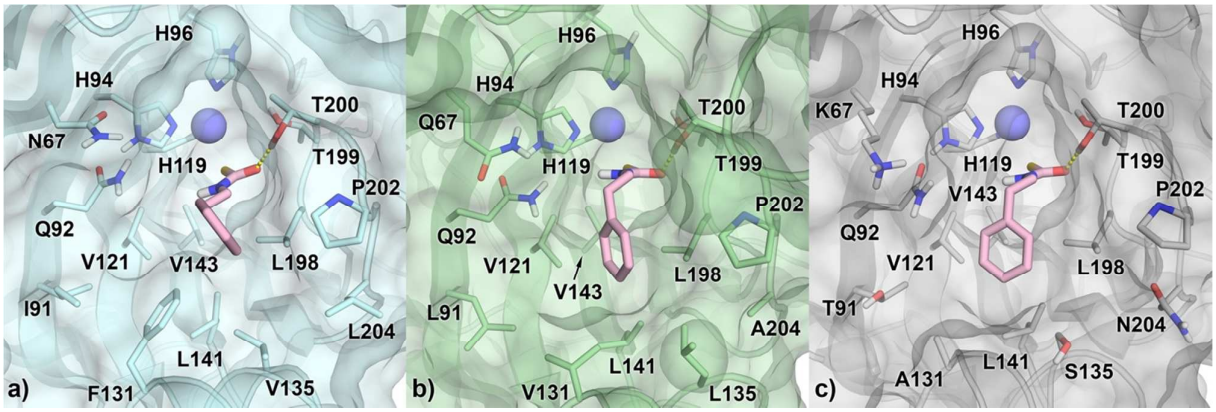

Figure 2. Binding mode of compound **2a** at the active site of **a**) hCA II (PDB code 3P5L), [23a] **b**) hCA IX (PDB code 3IAI) [1e] and **c**) hCA XII (PDB code 1JD0).[1f] The ligand is shown as pink sticks. hCA II, IX and XII are represented as surface and cartoons, respectively. Amino acids important for

ligand binding are highlighted as sticks. The Zn^{2+} ion is depicted as a purple sphere. Hydrogen bonds are displayed as dashed yellow lines.

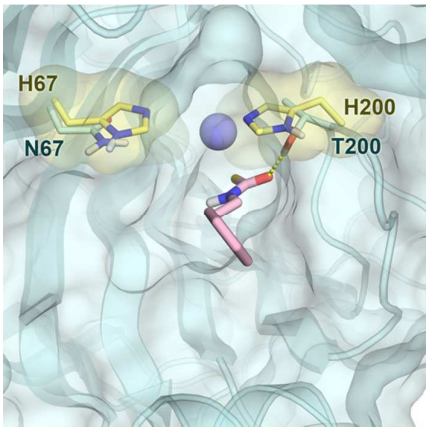

Figure 3. Superposition between the predicted hCA II-**2a** complex and the crystal structure of hCA I (PDB code 2NMX).[27] The ligand is shown as pink sticks. hCA II and I (only key substitutions) are represented as cyan and yellow cartoon and surfaces, respectively. In both enzymes, residues important for selectivity are highlighted as sticks. The Zn^{2+} ion is depicted as a purple sphere. Hydrogen bonds are displayed as dashed yellow lines.

IOP lowering activity.

The main clinical approach for the treatment of glaucoma or glaucoma related diseases, consists in tackling the intra-ocular-pressure (IOP) increase, which is the typical symptom. Nowadays such a result can be achieved through laser therapy or surgical operation. However, the preferred way still remains the topical pharmacological administration of drugs comprising para/sympaticomimetics, β-blockers and CAIs alone or in combination. [8-10]The use of CAIs, such as Dorzolamide or Brinzolamide, is by far the most common since their lesser side effects allow for chronic treatments.[8-10] Among the MTC series herein reported, we investigated some of the most active compounds against the hCA II (**2a, 3a, 11a** and **15a**) for their IOP lowering ability *in vivo*. Such

compounds were considered also for their excellent water solubility properties. All MTCs were formulated at 1% eye drop solution at neutral pH (due to their salt character), whereas the standard Dorzolamide was formulated at pH 5.5, as a hydrochloride salt. The water solubility of eye drugs is usually a problem of particular relevance. Actually the majority of drugs used for the topical treatment of glaucoma usually possess acceptable solubility for the obtainment of the pharmacological effect only as salts with strong acids, thus causing eye irritation and Dorzolamide is a well-known case.[7-10]

In our experiments we induced a transient ocular hypertention by the injection of 50 µl of sterile hypertonic saline in the vitreous of New Zealand white rabbits, then the MTCs were administered and compared both to the clinically used **DRZ** and vehicle (**Figure 4**).

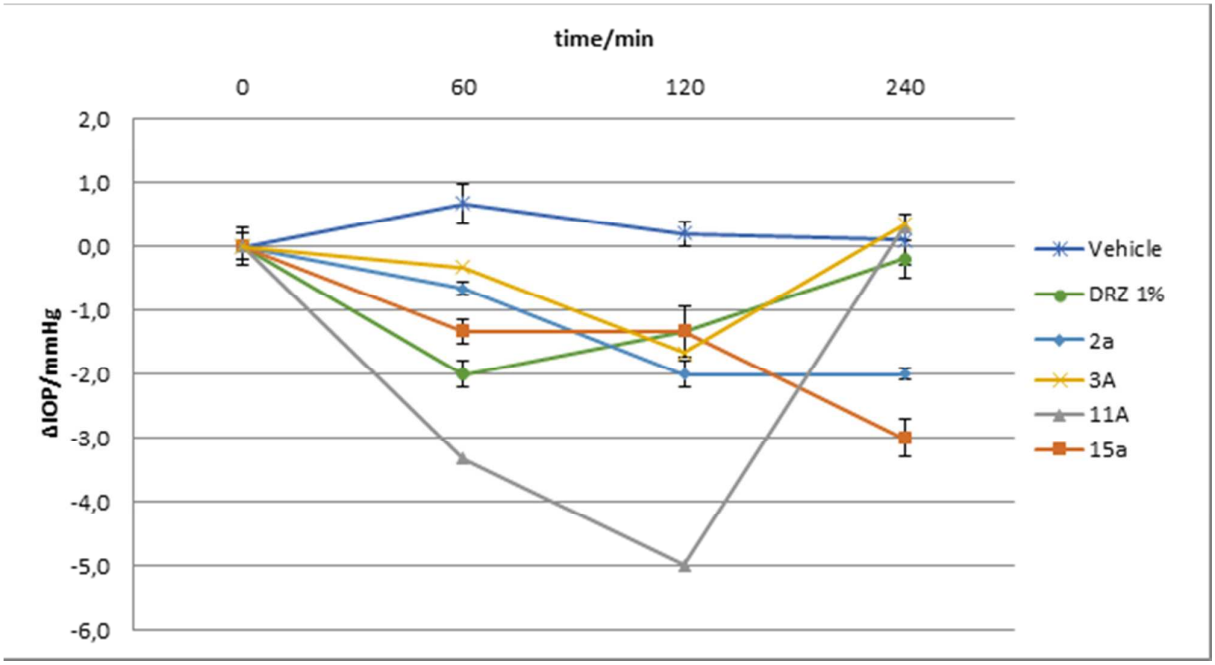

Figure 4. Intraocular pressure (ΔIOP, in mmHg) lowering *versus* time (min) of hypertonic saline-induced ocular hypertension in rabbits, treated with 50 µL of 1% solution of compounds **2a, 3a, 11a** and **15a** using **DRZ** as standard drug and vehicle. Errors were within 10-15% of the reported IOP values (from three different measurements for each of the four animals in the study group) and were statistically significant ($p = 0.045$ by the Student's t test)

As reported above all the compounds tested clearly showed IOP reduction potencies up to 120 minutes. In particular the MTC **11a** showed the strongest biological effect already at 60 minutes after injection (3.8 mmHg ΔIOP) and reached the maximum up to 120 minutes (4.9 mmHg ΔIOP). The Hexaprazole MTC **15a** provided an IOP reducing outcome comparable to the standard Dorzolamide up to 120 minutes and then its effect resulted increased over the time of the experiment (data not shown). In analogy the MTC **2a** showed an IOP reducing pattern similar to Dorzolamide even if lower in magnitude. Interestingly **2a** and **15a** retained their IOP reduction activities up to 240 minutes. Compound **3a** didn't show significant IOP lowering ability and reached its maximum at 120 minutes with ΔIOP value comparable to the standard Dorzolamide.

Conclusions

We report for the first time MTCs as a new class of CAIs. All compounds **1a-15a** were prepared according to known reported synthetic methods and characterized by means of spectroscopic, mass and elemental analyses. The MTCs were evaluated for their ability to inhibit the most relevant physio/pathological hCA isoforms (I, II, IX and XII) *in vitro.* They exhibited K_I values comprised between the low and medium nanomolar range. Noteworthy the MTCs reported here were highly potent against the transmembrane isoforms hCA IX and XII. Molecular modeling studies elucidated the binding mode of our inhibitors to the distinct hCA isoforms, thus revealing at the molecular bases their different activity and selectivity profiles.

The best performing compounds against the highly abundant hCA II isoform and showing excellent aqueous solubility properties, were tested in an acute glaucoma animal model for their ability to lower the IOP values in comparison to the standard drug Dorzolamide at the same concentrations. Interestingly the Hexaprazole MTC **11a** was the most potent in lowering the IOP but within a short period (120 min), whereas **2a** and **15a** were respectively able to retain their biological response up

to 240 minutes. Thus we can consider the MTCs as a new class of CAIs which may constitute interesting candidates for the future development of novel antiglaucoma drugs, a field in which no new drug has emerged in the last 15 years. Moreover our study reports on an unusual zinc binding motif the medicinal chemistry field, the MTCs, which can be successfully considered for its activity on different metalloenzymes of pharmaceutical interest.

Experimental protocols

General. Anhydrous solvents and all reagents were purchased from Sigma-Aldrich, Alfa Aesar and TCI. All reactions involving air- or moisture-sensitive compounds were performed under a nitrogen atmosphere using dried glassware and syringes techniques to transfer solutions. Nuclear magnetic resonance (^{1}H-NMR, ^{13}C-NMR) spectra were recorded using a Bruker Advance III 400 MHz spectrometer in DMSO-d_6. Chemical shifts are reported in parts per million (ppm) and the coupling constants (*J*) are expressed in Hertz (Hz). Splitting patterns are designated as follows: s, singlet; d, doublet; t, triplet; m, multiplet; brs, broad singlet; dd, double of doubles. The assignment of exchangeable protons (O*H* and N*H*) was confirmed by the addition of D_2O. Analytical thin-layer chromatography (TLC) was carried out on Merck silica gel F-254 plates. Flash chromatography purifications were performed on Merck Silica gel 60 (230-400 mesh ASTM) as the stationary phase and MeOH/DCM were used as eluents. Melting points (m.p.) were carried out in open capillary tubes and are uncorrected. ESI-MS spectra were recorded by direct introduction at 5 mL/min flow rate in an LTQ linear ion trap (Thermo, San Jose, CA, USA), equipped with a conventional ESI source. The spectra were acquired in both positive and negative ion mode; the specific conditions used for these experiments were as follows: the spray voltage was 5 kV in both polarity; the capillary voltage were 49 V in positive ion mode and -15 V in negative ion mode; the capillary temperature was kept at 280C. The sheath gas was set at 10 (arbitrary units), the sweep gas and auxiliary gas were kept at 5 (arbitrary units). Scan Time was 2 microscans and the maximun

injection time was 50ms. The ESI spectra were acquired using Xcalibur 2.0 (Thermo) the spectrum range was 150-500 m/z. A Gallenkamp MPD350.BM3.5 apparatus was used to measure the melting points.Amines **1-15** were commercially available (from Sigma-Aldrich, Milan, Italy). All compounds reported **1a-15a** were >98% pure by HPLC

General procedure for the synthesis of monothiocarbamates 1a-15a.[28]

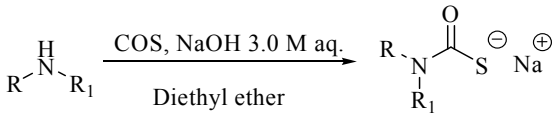

1-15 **1a-15a**

The appropriate amines **1-15** (1.0 eq.) were dissolved in diethyl ether and treated with a freshly prepared 3.0 M aqueous solution of NaOH (1.2 eq). The mixture was stirred at r.t. for 10 minutes, then freshly produced COS was bubbled until the formation of a heavy precipitate. The reaction mixture was stirred for 10 min and then all solvents were removed under *vacuo* to give a solid residue, which was dissolved in MeOH and filtered through a Celite pad. The filtrate was concentrated under *vacuo* to afford the titled compounds **1a-15a**.

Synthesis of Carbonyl Sulfide (COS).[28]

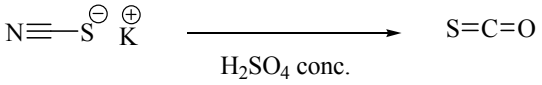

COS was generated by modification of the procedures reported in the literature.[28] A saturated aqueous solution of potassium thiocyanate was carefully added through a pressure equalized dropping funnel to a concentrate sulfuric acid solution at –15 °C contained into an Erlenmeyer

flask. The gas evolved was purified by bubbling into a 33% aqueous sodium hydroxide and concentrated sulfuric acid solutions prior to be injected into the reaction vessel.

Synthesis of 3,4-dimethoxyphenethylcarbamothioate sodium salt **1a**.

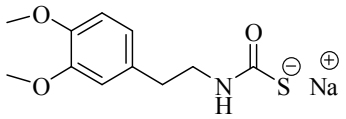

1a

3,4-Dimethoxyphenethylcarbamothioate sodium salt **1a** was obtained according to the general procedure previously reported using 2-(3',4'-dimethoxyphenyl)ethanamine **1**.

3,4-Dimethoxyphenethylcarbamothioate sodium salt **1a**: 72% yield; δ_H (400 MHz, DMSO-d_6) 2.73 (2H, d, *J* 6.7, CH_2), 3.12 (2H, d, *J* 6.7, CH_2NH), 3.74 (3H, s, OCH_3), 3.76 (3H, s, OCH_3), 6.72 (1H, appt, *J* 7.8, Ar*H*), 6.81 (1H, m, Ar*H*), 6.88 (1H, d, *J* 7.8, Ar*H*); δ_C(100 MHz, DMSO-d_6) 36.7, 44.7, 56.5, 56.6, 113.0, 113.6, 121.4, 134.0, 148.1, 149.6, 184.4; Elemental analysis: calc: C, 50.18; H, 5.36; N, 5.32; S, 12.18; found: C, 50.20; H, 5.40; N, 5.35; S, 12.14; *m/z* (ESI negative) 240.07 [M-Na]$^-$.

Synthesis of phenethylcarbamothioate sodium salt **2a**.

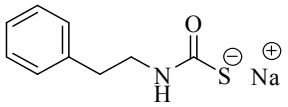

2a

Phenethylcarbamothioate sodium salt **2a** was obtained according to the general procedure previously reported using 2-phenylethanamine **2**.

Phenethylcarbamothioate sodium salt **2a**: 65% yield; δ_H (400 MHz, DMSO-d_6) 2.74 (2H, d, *J* 6.8, CH_2), 3.14 (2H, d, *J* 6.8, CH_2NH), 7.27 (2H, d, *J* 7.8, Ar*H*), 7.31 (2H, d, *J* 7.8, Ar*H*), 7.38 (1H, appt, *J* 7.8, Ar*H*); δ_C(100 MHz, DMSO-d_6) 36.6, 45.8, 123.0, 134.0, 146.2, 148.8, 185.0; Elemental analysis: calc: C, 53.19; H, 4.96; N, 6.89; S, 15.78; found: C, 53.17; H, 4.98; N, 6.87; S, 15.74; *m/z* (ESI negative) 180.05 $[M-Na]^-$.

Synthesis of 4-methylpiperazin-1-ylcarbamothioate sodium salt **3a**.

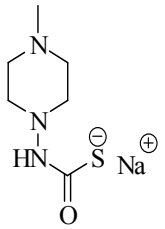

3a

4-Methylpiperazin-1-ylcarbamothioate sodium salt **3a** was obtained according to the general procedure previously reported using 4-methylpiperazin-1-amine **3**.

4-Methylpiperazin-1-ylcarbamothioate sodium salt **3a**: 60% yield; δ_H (400 MHz, DMSO-d_6) 2.32 (3H, s, CH_3), 2.52 (4H, m, 2 x CH_2), 2.63 (4H, m, 2 x CH_2); δ_C(100 MHz, DMSO-d_6) 44.2, 54.2, 56.9, 184.9; Elemental analysis: calc: C, 36.54; H, 6.13; N, 21.30; S, 16.26; found: C, 36.56; H, 6.12; N, 21.28; S, 16.22; *m/z* (ESI negative) 174.07 $[M-Na]^-$.

Synthesis of *N,N*-dipropylcarbamothioate sodium salt **4a**.

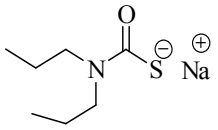

4a

N,N-Dipropylcarbamothioate sodium salt **4a** was obtained according to the general procedure previously reported using *N,N*-dipropylamine **4**.

N,N-Dipropylcarbamothioate sodium salt **4a**: 60% yield; δ_H (400 MHz, DMSO-d_6) 0.92 (3H, t, *J* 6.8, CH_3), 1.00 (3H, t, *J* 6.8, CH_3), 1.48 (4H, m, 2 x CH_2), 2.63 (4H, m, 2 x CH_2); δ_C(100 MHz, DMSO-d_6) 15.2, 18.6, 52.4, 185.1; Elemental analysis: calc: C, 45.88; H, 7.70; N, 7.64; S, 17.50; found: C, 46.01; H, 7.74; N, 7.58; S, 17.46; *m/z* (ESI negative) 160.08 $[M-Na]^-$.

Synthesis of *N,N*-dibutylcarbamothioate sodium salt **5a**.

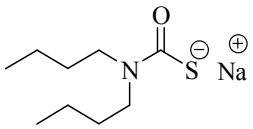

5a

N,N-Dibutylcarbamothioate sodium salt **5a** was obtained according to the general procedure previously reported using *N,N*-dibutylamine **5**.

N,N-Dibutylcarbamothioate sodium salt **5a**: 58% yield; δ_H (400 MHz, DMSO-d_6) 0.98 (3H, t, *J* 6.8, CH_3), 1.00 (3H, t, *J* 6.8, CH_3), 1.32 (4H, m, 2 x CH_2), 1.50 (4H, m, 2 x CH_2), 2.69 (4H, m, 2 x CH_2); δ_C(100 MHz, DMSO-d_6) 15.2, 18.6, 52.4, 185.1; δ_C(100 MHz, DMSO-d_6) 14.8, 15.0, 20.2, 27.8, 47.9, 184.6; Elemental analysis: calc: C, 51.16; H, 8.59; N, 6.63; S, 15.18; found: C, 51.14; H, 8.55; N, 6.60; S, 15.14; *m/z* (ESI negative) 188.11 $[M-Na]^-$.

Synthesis of *N,N*-diisobutylcarbamothioate sodium salt **6a**.

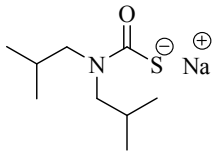

6a

N,N-Diisobutylcarbamothioate sodium salt **6a** was obtained according to the general procedure previously reported using *N,N*-diisobutylamine **6**.

N,N-Diisobutylcarbamothioate sodium salt **6a**: 32% yield; m.p. 214°C (Lit. [29]: 210-212°C; δ_H (400 MHz, DMSO-d_6) 0.96 (12H, m, 4 x CH_3), 2.56 (2H, m, 2 x C*H*), 2.73 (4H, d, *J* 6.8, 2 x CH_2); δ_C(100 MHz, DMSO-d_6) 21.3, 27.8, 51.9, 186.0; Elemental analysis: calc: C, 51.16; H, 8.59; N, 6.63; S, 15.18; found: C, 51.18; H, 8.62; N, 6.58; S, 15.02; *m/z* (ESI negative) 211.10 $[M-Na]^-$.

Synthesis of *N,N*-butyl(ethyl)carbamothioate sodium salt **7a**.

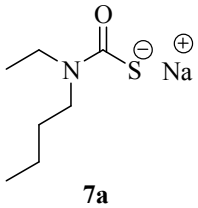

7a

N,N-Butyl(ethyl)carbamothioate sodium salt **7a** was obtained according to the general procedure previously reported using *N*-ethylbutan-1-amine **7**.

N,N-Butyl(ethyl)carbamothioate sodium salt **7a**: 66% yield; δ_H (400 MHz, DMSO-d_6) 0.90 (3H, t, *J* 6.8, CH_3), 1.01 (3H, t, *J* 6.8, CH_3), 1.24 (2H, m, CH_2), 1.48 (2H, m, CH_2), 3.40 (4H, m, 2 x CH_2); δ_C(100 MHz, DMSO-d_6) 14.7, 15.0, 20.8, 31.6, 48.8, 180.8; Elemental analysis: calc: C, 45.88; H, 7.70; N, 7.64; S, 17.50; found: C, 45.90; H, 7.72; N, 7.68; S, 17.44; *m/z* (ESI negative) 160.08 $[M-Na]^-$.

Synthesis of ethyl-*N*-oxoethylmethylcarbamothioate sodium salt **8a**.

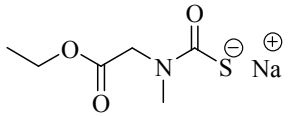

8a

Ethyl-*N*-oxoethylmethylcarbamothioate sodium salt **8a** was obtained according to the general procedure previously reported using ethyl 2-(methylamino)acetate **8**.

Ethyl-*N*-oxoethylmethylcarbamothioate sodium salt **8a**: 22% yield; δ_H (400 MHz, DMSO-d_6) 1.27 (3H, t, *J* 6.4, CH_2CH_3), 2.82 (3H, s, NCH_3), 3.95 (2H, s, CH_2), 4.28 (2H, q, *J* 6.4, CH_2CH_3); δ_C(100 MHz, DMSO-d_6) 13.8, 36.7, 54.2, 63.0, 168.8, 185.4; Elemental analysis: calc: C, 36.18; H, 5.06; N, 7.03; S, 16.10; found: C, 36.20; H, 5.09; N, 7.00; S, 16.07; *m/z* (ESI negative) 176.04 $[M-Na]^-$.

Synthesis of *N*-benzyl-*N*-methylcarbamothioate sodium salt **9a**.

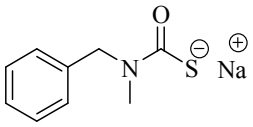

9a

N-Benzyl-*N*-methylcarbamothioate sodium salt **9a** was obtained according to the general procedure previously reported using *N*-methyl(phenyl)methanamine **9**.

N-Benzyl-*N*-methylcarbamothioate sodium salt **9a**: 32% yield; δ_H (400 MHz, DMSO-d_6) 3.10 (3H, s, CH_3), 4.20 (2H, s, CH_2), 7.23 (1H, appt, *J* 8.4, Ar*H*), 7.31 (2H, d, *J* 8.4, Ar*H*), 7.28 (2H, d, *J* 8.4, Ar*H*); δ_C(100 MHz, DMSO-d_6) 33.2, 55.6, 127.2, 128.3, 129.0, 141.4, 186.3; Elemental analysis: calc: C, 53.19; H, 4.96; N, 6.89; S, 15.78; found: C, 53.17; H, 4.94; N, 6.88; S, 15.75; *m/z* (ESI negative) 180.05 $[M-Na]^-$.

Synthesis of morpholine-4-carbothioate sodium salt **10a**.

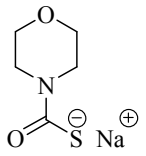

10a

Morpholine-4-carbothioate sodium salt **10a**was obtained according to the general procedure previously reported using morpholine **10**.

Morpholine-4-carbothioate sodium salt **10a**: 82% yield; δ_H (400 MHz, DMSO-d_6) 2.67 (4H, m, CH_2), 3.3.53 (4H, m, 2 x CH_2); δ_C(100 MHz, DMSO-d_6) 45.9, 68.3, 185.3; Elemental analysis: calc: C, 35.50; H, 4.77; N, 8.28; S, 18.95; found: C, 35.52; H, 4.76; N, 8.30; S, 18.92; *m/z* (ESI negative) 146.03 $[M-Na]^-$.

Synthesis of piperazine-1,4-carbothioate sodium salt **11a**.

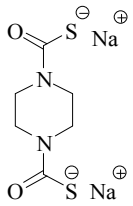

11a

Piperazine-1,4-carbothioate sodium salt **11a** was obtained according to the general procedure previously reported using piperazine **11**.

Piperazine-1,4-carbothioate sodium salt **11a**: 38% yield; δ_H (400 MHz, DMSO-d_6) 4.80 (8H, brs, 4 x CH_2); δ_C(100 MHz, DMSO-d_6) 46.9, 185.2; Elemental analysis: calc: C, 38.28; H, 4.28; N, 14.88; S, 34.06; found: C, 38.25; H, 4.30; N, 14.86; S, 34.01; *m/z* (ESI negative) 188.01 $[M-Na]^-$.

Experimental data in agreement with reported data. [30]

Synthesis of 4-(4-fluorophenyl)piperazine-1-carbothioate sodium salt **12a**.

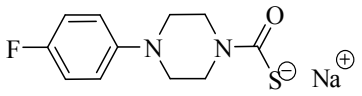

12a

4-(4-Fluorophenyl)piperazine-1-carbothioate sodium salt **12a** was obtained according to the general procedure previously reported using 1-(4-fluorophenyl)piperazine **12**.

4-(4-Fluorophenyl)piperazine-1-carbothioate sodium salt **12a**: 56% yield; δ_H (400 MHz, DMSO-d_6) 2.86 (4H, m, 2 x CH_2), 3.81 (4H, brs, 2 x CH_2), 6.94 (2H, m, ArH), 7.19 (2H, m, ArH); δ_C(100 MHz, DMSO-d_6) 45.3, 50.7, 116.1 (d, $J^2_{C\text{-}F}$ 22.0), 118.5, 149.5, 156.0 (d, $J^1_{C\text{-}F}$ 234), 185.0; δ_F(376.6 MHz, DMSO-d_6) -125.75 (1F, s); Elemental analysis: calc: C, 50.37; H, 4.61; N, 10.68; S, 12.23; found: C, 50.40; H, 4.59; N, 10.66; S, 12.19; *m/z* (ESI negative) 239.07 $[M\text{-}Na]^-$.

Synthesis of 4-(4-trifluorophenyl)piperazine-1-carbothioate sodium salt **13a**.

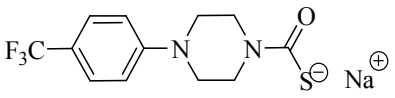

13a

4-(4-Trifluorophenyl)piperazine-1-carbothioate sodium salt **13a** was obtained according to the general procedure previously reported using 1-(4-trifluorophenyl)piperazine **13**.

4-(4-Trifluorophenyl)piperazine-1-carbothioate sodium salt **13a**: 48% yield; δ_H (400 MHz, DMSO-d_6) 2.84 (4H, m, 2 x CH_2), 3.79 (4H, brs, 2 x CH_2), 6.96 (2H, m, ArH), 7.22 (2H, m, ArH); δ_C(100 MHz, DMSO-d_6) 45.7, 48.3, 115.1, 118.3 (q, $J^2_{C\text{-}F}$ 31.0), 126.0 (d, $J^1_{C\text{-}F}$ 270), 127.3, 154.4, 185.0;

δ_F(376.6 MHz, DMSO-d_6) -59.9 (1F, s); Elemental analysis: calc: C, 46.15; H, 3.87; N, 8.97; S, 10.27; found: C, 46.18; H, 3.89; N, 8.95; S, 10.24; *m/z* (ESI negative) 289.06 [M-Na]$^-$.

Synthesis of 4-(3-chlorophenyl)piperazine-1-carbothioate sodium salt **14a**.

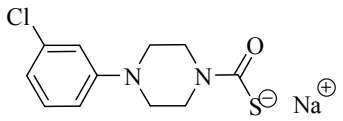

14a

4-(3-Chlorophenyl)piperazine-1-carbothioate sodium salt **14a** was obtained according to the general procedure previously reported using 4-(3-chlorophenyl)piperazine **14**.

4-(3-Chlorophenyl)piperazine-1-carbothioate sodium salt **14a**: 70% yield; δ_H (400 MHz, DMSO-d_6) 3.06 (4H, t, *J* 6.8, 2 x CH_2), 3.80 (4H, brs, 2 x CH_2), 6.78 (1H, d *J* 8.4, Ar*H*), 6.93 (2H, m, Ar*H*), 7.23 (1H, appt, *J* 8.4, Ar*H*); δ_C(100 MHz, DMSO-d_6) 46.4, 49.7, 114.4, 115.6, 118.8, 131.3, 134.7, 153.5, 185.4; Elemental analysis: calc: C, 45.88; H, 7.70; N, 7.64; S, 17.50; found: C, 45.90; H, 7.72; N, 7.68; S, 17.44; *m/z* (ESI negative) 160.08 [M-Na]$^-$.

Synthesis of 4-(2-(cyclohexylamino)-2-oxoethyl)piperazine-1-carbothioate sodium salt **15a**.

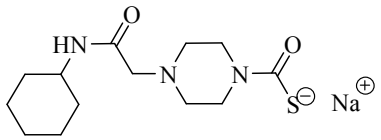

15a

4-(2-(Cyclohexylamino)-2-oxoethyl)piperazine-1-carbothioate sodium salt **15a** was obtained according to the general procedure previously reported using 4-(2-(cyclohexylamino)-2-oxoethyl)piperazine **15**.

4-(2-(Cyclohexylamino)-2-oxoethyl)piperazine-1-carbothioate sodium salt **15a**: 54% yield; δ_H (400 MHz, DMSO-d_6) 1.18 (4H, m), 1.38 (4H, m), 1.56 (2H, m), 2.65 (4H, m), 3.14 (4H, m), 3.36 (2H,

s, CH2), 3.52 (1H, m); δ_C (100 MHz, DMSO-d_6) 25.4, 26.1, 33.2, 46.4, 47.8, 54.2, 62.4, 169.0, 185.0; Elemental analysis: calc: C, 50.80; H, 7.21; N, 13.67; S, 10.43; found: C, 50.81; H, 7.23; N, 13.65; S, 10.40; *m/z* (ESI negative) 284.14 $[M-Na]^-$.

CA Inhibition

An Applied Photophysics stopped-flow instrument has been used for assaying the CA-catalyzed CO_2 hydration activity. Phenol red (at a concentration of 0.2 mM) has been used as a pH indicator, working at the absorbance maximum of 557 nm, with 20 mM Hepes (pH 7.5) as the buffer, and 20 mM Na_2SO_4 (for maintaining constant the ionic strength), following the initial rates of the CA-catalyzed CO_2 hydration reaction for a period of 10−100 s.[25] The CO_2 concentrations ranged from 1.7 to 17 mM for the determination of the kinetic parameters and inhibition constants. For each inhibitor, at least six traces of the initial 5−10 % of the reaction have been used for determining the initial velocity. The uncatalyzed rates were determined in the same manner and subtracted from the total observed rates. Stock solutions of inhibitor (0.1 mM) were prepared in distilled−deionized water, and dilutions up to 0.01 nM were done thereafter with distilled−deionized water. Inhibitor and enzyme solutions were preincubated together for 15 min at room temperature prior to assay, to allow for the formation of the E−I complex. The inhibition constants were obtained by nonlinear least squares methods using PRISM 3, as reported earlier,[20] and represent the mean from at least three different determinations. All CA isofoms were recombinant ones obtained in house as reported earlier.[20-24]

Molecular Modelling.

Ligand setup. The ligand's tridimensional structures were generated with Maestro v. 10.4 (Maestro, version 10.4, Schrödinger, LLC, New York, NY, 2015). Protonation states, including the

potential metal-binding forms, were predicted using Epik 3.4 as implemented in Maestro (Epik, version 3.4, Schrödinger, LLC, New York, NY, 2015). Ligands geometry were then optimized through a Polak−Ribiere conjugate gradient minimization (convergence = 0.0005 kJ $Å^{-1}$ mol^{-1}) using the MacroModel v.11.0 module in Maestro (MacroModel, version 11.0, Schrödinger, LLC, New York, NY, 2015). Due to the inaccuracies in the assignment of partial charges of the MTC moiety by the empirical force fields implemented in Maestro, ligands charges were computed using the Restrained Electrostatic Potential (RESP) fitting procedure. [31] The ESP was first calculated with Gaussian 09 Rev. D.01 (Gaussian 09, Revision E.01, Gaussian, Inc., Wallingford CT, 2009) using a 6–31G* basis set at the Hartree–Fock level of theory, and then the RESP charges were obtained by a two-stages fitting procedure using Antechamber.[32]

Proteins setup. The crystal structures of hCA II (PDB code 3P5L),[23a] and of the catalytic domains of hCA IX (PDB code 3IAI)[1e] and hCA XII (PDB code 1JD0)[1f] were prepared for docking calculations using the "Protein Preparation Wizard" panel of Schrödinger 2015 molecular modeling package (Maestro, version 10.4, Schrödinger, LLC, New York, NY, 2015). First, missing side chains or loops were added using Prime 4.2 (Prime, version 4.2, Schrödinger, LLC, New York, NY, 2015). Then, bond orders were assigned and all the hydrogen atoms were added. The prediction of the side chains hetero groups ionization and tautomeric states was performed using Epik 3.4 (Epik, version 3.4, Schrödinger, LLC, New York, NY, 2015). Finally, an optimization of the hydrogen-bonding network was performed, and the positions of the hydrogen atoms were optimized. All the water molecules were deleted prior to docking calculations.

Molecular docking. Docking studies were carried out with the grid-based program Glide 6.9.[33] For the grid generation, a box of 22Å x 22Å x 22Å, surrounding the ligand binding cavity site, was considered for each enzyme. The standard precision (SP) mode of the GlideScore function was used to score the predicted binding poses. The force field used for the docking was OPLS-2005.[34] All of the pictures were rendered with PyMOL (www.pymol.org).

Transient ocular hypertensive rabbit model.

The increase in IOP was induced by the injection of 50 μl of sterile hypertonic saline (5%) into the vitreous bilaterally in pre-anesthetized New Zealand white rabbits with tiletamine/zolazepam (Zoletil 50/50 mg/mL, Virbac) i.m. 0.05 ml/kg, plus xylazine (Xylor 2%,) i.m. 0.02 ml/kg.[10d] Drugs were dissolved in pirogen-free appropriate vehicle (buffered aqueous solution pH 7, polyoxyl 40, dimethylsulphoxyde (DMSO) 2%, hydrogenated castor oil 5 mg/ml, tromethamine 10 mg/ml, edetate disodium 0.5mg/ml and benzalkonium chloride 0.15 mg/mL) and administered as eye drops at different concentrations immediately after hypertonic saline injection. IOP was measured using a Tono-Pen AVIA® (Reichert Inc. Depew, NY) prior (basal) and post hypertonic saline injection 60, 120, 240 min after drug or vehicle treatment. One drop of 0.2% oxybuprocaine hydrochloride, 4 mg/ml, was instilled in each eye immediately before each set of pressure measurements. The ocular hypotensive activity of studied compounds is expressed in mmHg as average difference in IOP between drug- and vehicle-treated eyes.[10d]

Acknowledgements. This research was financed by two EU grants of the 7th framework program (Metoxia and Dynano projects to AS and CTS).

Corresponding Authors. FC, Phone: +39-055-4573005; fax: +39-055-4573385; E-mail: fabrizio.carta@unifi.it; CTS, Phone: +39-055-4573005; fax: +39-055-4573385; E-mail: claudiu.supuran@unifi.it

Abbreviations Used. MTCs, monothiocarbamates; CAI(s), carbonic anhydrase inhibitor(s); AAZ, acetazolamide; (h)CA, (human)carbonic anhydrase; K_I, inhibition constant;

Supporting Informations. Supporting Informations are available free of charge on the ACS Publications website. Superposition of a predicted binding pose of compound **2a** with a known DTC at the hCA II active site (**Figure S1**), binding mode of compounds **4a**, **11a** and **12a** at the active site of hCA II (**Figure S2**), multiple sequence alignment of hCA I, II, IX and XII (**Figure S3**) and molecular formula strings.

References.

(1) (a) Krishnamurthy, V. M.; Kaufman, G. K.; Urbach, A. R.; Gitlin, I.; Gudiksen, K. L.; Weibel, D. B.; Whitesides, G. M. Carbonic anhydrase as a model for biophysical and physical-organic studies of proteins and protein-ligand binding. *Chem. Rev*. **2008**, *108*, 946−1051. (b) Lou, Y.; McDonald, P. C.; Oloumi, A.; Chia, S.; Ostlund, C.; Ahmadi, A.; Kyle, A.; Auf dem Keller, U.; Leung, S.; Huntsman, D.; Clarke, B.; Sutherland, B. W.; Waterhouse, D.; Bally, M.; Roskelley, C.; Overall, C. M.; Minchinton, A.; Pacchiano, F.; Carta, F.; Scozzafava, A.; Touisni, N.; Winum, J. Y.; Supuran, C. T.; Dedhar, S. Targeting tumor hypoxia: suppression of breast tumor growth and metastasis by novel carbonic anhydrase IX inhibitors. *Cancer Res.* **2011,** *71*, 3364-3376; (c) Supuran, C. T. Carbonic anhydrases: novel therapeutic applications for inhibitors and activators. *Nat. Rev. Drug Disc.* **2008**, *7*, 168−181. (d) Tanc, M.; Carta, F.; Scozzafava, A.; Supuran, C.T. α-Carbonic anhydrases possess thioesterase activity. *ACS Med Chem Lett*. **2015**, *6*, 292-295. (e) Alterio, V.; Hilvo, M.; Di Fiore, A.; Supuran, C. T.; Pan, P.; Parkkila, S.; Scaloni, A.; Pastorek, J.; Pastorekova, S.; Pedone, C.; Scozzafava, A.; Monti, S. M.; De Simone, G. Crystal structure of the catalytic domain of the tumor-associated human carbonic anhydrase IX. *Proc. Natl. Acad. Sci. U. S. A.* **2009**, *106*, 16233–16238. (f) Whittington, D. A.; Waheed, A.; Ulmasov, B.; Shah, G. N.; Grubb, J. H.; Sly, W. S.; Christianson, D. W. Crystal structure of the dimeric extracellular domain of human carbonic anhydrase XII, a bitopic membrane protein overexpressed in certain cancer tumor cells. *Proc. Natl. Acad. Sci. U. S. A.* **2001**, *98*, 9545–9550.

(2) (a) Supuran, C. T.; Scozzafava, A.; Casini, A. Carbonic anhydrase inhibitors. *Med. Res. Rev*. **2003**, *23*, 146-189. (b) Pastorekova, P. S.; Pastorek, J.; Supuran, C. T. Carbonic anhydrases: Current state of the art, therapeutic applications and future prospects. *J. Enzyme Inhib. Med. Chem*. **2004**, *19*, 199−229. (c) Thiry, A.; Dogné, J.-M.; Masereel, B.; Supuran, C. T. Targeting tumor-associated carbonic anhydrase IX in cancer therapy. *Trends Pharmacol. Sci*. **2006**, *27*, 566−573.

(3) (a) Supuran, C. T. Carbonic anhydrase inhibitors. *Bioorg. Med. Chem. Lett*. **2010**, *20*, 3467−3474. (b) Supuran, C. T. Carbonic anhydrase inhibitors and activators for novel therapeutic applications. *Future Med. Chem*. **2011**, *3*, 1165−1180. (c) Nishimori, I.; Minakuchi, T.; Maresca, A.; Carta, F.; Scozzafava, A.; Supuran, C. T. The β-carbonic anhydrases from Mycobacterium tuberculosis as drug targets. *Curr. Pharm. Des*. **2010**, *16*, 3300−3309. (d) Carta, F.; Supuran, C.T.; Scozzafava, A. Sulfonamides and their isosters as carbonic anhydrase inhibitors. *Future Med Chem*. **2014**, *6*, 1149-1165. (e) Supuran, C. T. Carbonic anhydrase inhibitors. *Bioorg. Med. Chem. Lett*. **2010**, *20*, 3467−3474.

(4) (a) Supuran, C. T. Structure and function of carbonic anhydrases. *Biochem. J*. **2016**, in press (doi: 10.1042/BCJ20160115); (b) Supuran, C.T. Inhibition of carbonic anhydrase IX as a novel anticancer mechanism. *World J. Clin. Oncol.* **2012**, *3*, 98-103; (c) De Simone, G.; Supuran, C.T. Carbonic anhydrase IX: biochemical and crystallographic characterization of a novel antitumor target. *Biochim. Biophys. Acta* **2010**, *1804*, 404-409.

(5) (a) Supuran, C. T.; Casini, A.; Scozzafava, A. In Carbonic Anhydrase: Its Inhibitors and Activators; Supuran, C. T., Scozzafava, A., Conway, J., Eds.; CRC Press: Boca Raton, FL, 2004; p 67; (b) De Simone, G.; Alterio, V.; Supuran, C.T. Exploiting the hydrophobic and hydrophilic binding sites for designing carbonic anhydrase inhibitors. *Expert Opin. Drug Discov*. **2013**, *8*, 793-810.

(6) (a) Aggarwal, M.; Kondeti, B.; McKenna, R. Anticonvulsivant/antiepileptic carbonic anhydrase inhibitors: a patent review. *Expert Opin. Ther. Pat*. **2013**, *23*, 717−724. (b) Aggarwal, M.; Boone, C. D.; Kondeti, B.; McKenna, R. Structural annotation of human carbonic anhydrases. *J. Enzyme Inhib. Med. Chem*. **2013**, *28*, 267−277.

(7) Supuran, C. T. Carbonic anhydrases: from biomedical applications of the inhibitors and activators to biotechnologic use for CO_2 capture. *J. Enzyme Inhib. Med. Chem*. **2013**, *28*, 229−230.

(8) (a) Sugrue, M. F. The pharmacology of antiglaucoma drugs. *Pharmacol. Ther*. **1999**, *43*, 91−138. (b) Carta, F.; Supuran, C. T.; Scozzafava, A. Novel therapies for glaucoma. A patent review 2007−2011. *Expert Opin. Ther. Pat*. **2012**, *22*, 79−88.

(9) (a) Mincione, F.; Scozzafava, A.; Supuran, C. T. The development of topically acting carbonic anhydrase inhibitors as antiglaucoma agents. *Curr. Pharm. Des*. **2008**, *14*, 649−654. (b) Masini, E.; Carta, F.; Scozzafava, A.; Supuran, C. T. Antiglaucoma carbonic anhydrase inhibitors: A patent review. *Expert Opin. Ther. Pat*. **2013**, *23*, 705−716. (c) Mincione, F.; Scozzafava, A.; Supuran, C. T. Antiglaucoma carbonic anhydrase inhibitors as ophthalomologic drugs. In Drug Design of Zinc-Enzyme Inhibitors: Functional, Structural, and Disease Applications; Supuran, C. T., Winum, J. Y., Eds.; Wiley: Hoboken, NJ, 2009; pp 139−154.

(10) (a) Steele, R. M.; Batugo, M. R.; Benedini, F.; Biondi, S.; Borghi, V.; Carzaniga, L.; Impagnatiello, F.; Maglietta, D.; Chong, W. K. M.; Rajapakse, R.; Cecchi, A.; Temperini, C.; Supuran, C. T. Nitric oxide donating carbonic anhydrase inhibitors for the treatment of open-angle glaucoma. *Bioorg. Med. Chem. Lett*. **2009**, *19*, 6565−6570. (b) Mincione, F.; Benedini, F.; Biondi, S.; Cecchi, A.; Temperini, C.; Formicola, G.; Pacileo, I.; Scozzafava, A.; Masini, E.; Supuran, C. T. Synthesis and crystallographic analysis of new sulfonamides incorporating NO-donating moieties with potent antiglaucoma action. *Bioorg. Med. Chem. Lett*. **2011**, *21*, 3216−3221. (c) Fabrizi, F.; Mincione, F.; Somma, T.; Scozzafava, G.; Galassi, F.; Masini, E.; Impagnatiello, F.; Supuran, C. T. A new approach to antiglaucoma drugs: carbonic anhydrase inhibitors with or without NO donating moieties. Mechanism of action and preliminary pharmacology. *J. Enzyme Inhib. Med. Chem*. **2012**, *27*, 138−147. (d) Borghi ,V.; Bastia, E.; Guzzetta, M.; Chiroli, V.; Toris, C.B.; Batugo, M.R.; Carreiro, S.T.; Chong, W.K.; Gale, D.C.; Kucera, D.J.; Jia, L.; Prasanna, G.; Ongini, E.; Krauss, A.H.; Impagnatiello, F. A novel nitric oxide releasing prostaglandin analog, NCX 125, reduces intraocular pressure in rabbit, dog, and primate models of glaucoma. *J. Ocul. Pharmacol. Ther.* **2010**, *26*, 125-132.

(11) (a) Supuran, C. T. How many carbonic anhydrase inhibition mechanisms exist? *J. Enzyme Inhib. Med. Chem.* **2016**, *31*, 345-360. (b) Carta, F.; Vullo, D.; Maresca, A.; Scozzafava, A.; Supuran, C.T. New chemotypes acting as isozyme-selective carbonic anhydrase inhibitors with low affinity for the offtarget cytosolic isoform II. *Bioorg Med Chem Lett*. **2012**, *22*, 2182-2185. (c) Scozzafava, A.; Supuran, C.T.; Carta, F. Antiobesity carbonic anhydrase inhibitors: a literature and patent review. *Expert Opin Ther Pat*. **2013**, *23*, 725-735.

(12) (a) Alterio, V.; Di Fiore, A.; D'Ambrosio, K.; Supuran, C. T.; De Simone, G. Multiple binding modes of inhibitors to carbonic anhydrases: how to design specific drugs targeting 15 different isoforms? *Chem. Rev*. **2012**, *112*, 4421−4468. (b) Supuran, C. T. Structure-based drug discovery of carbonic anhydrase inhibitors. *J. Enzyme Inhib. Med. Chem*. **2012**, *27*, 759−772.

(13) (a) Neri, D.; Supuran, C. T. Interfering with pH regulation in tumors as a therapeutic strategy. *Nat. Rev. Drug Discov.* **2011**, *10*, 767−777. (b) Gieling, R. G.; Parker, C. A.; De Costa, L. A.; Robertson, N.; Harris, A. L.; Stratford, I. J.; Williams, K. J. Inhibition of carbonic anhydrase activity modifies the toxicity of doxorubicin and melphalan in tumour cells in vitro. *J. Enzyme Inhib. Med. Chem*. **2013**, *28*, 360−369.

(14) (a) Capasso, C.; Supuran, C. T. Sulfa and trimethoprim-like drugs-antimetabolites acting as carbonic anhydrase, dihydropteroate synthase and dihydrofolate reductase inhibitors. *J. Enzyme Inhib. Med. Chem*. **2014**, *29*, 379−387. (b) Supuran, C. T. Bacterial carbonic anhydrases as drug targets: towards novel antibiotics? *Front. Pharmacol*. **2011**, *2*, 34. (c) Capasso, C.; Supuran, C. T. Antiinfective carbonic anhydrase inhibitors: a patent and literature review. *Expert Opin. Ther. Pat*. **2013**, *23*, 693−704.

(15) Ratto, F.; Witort, E.; Tatini, F.; Centi, S.; Lazzeri, L.; Carta, F.; Lulli, M.; Vullo, D.; Fusi, F.; Supuran, C. T.; Scozzafava, A.; Capaccioli, S.; Pini, R. Plasmonic particles that hit hypoxic cells. *Adv. Funct. Mater*. **2015**, *25*, 316−323.

(16) Dilworth, J. R.; Pascu, S. I.; Waghorn, P. A.; Vullo, D.; Bayly, S. R.; Christlieb, M.; Sun, X.; Supuran, C. T. Synthesis of sulfonamide conjugates of Cu(II), Ga(III), In(III), Re(V) and Zn(II)

complexes: carbonic anhydrase inhibition studies and cellular imaging investigations. *Dalton Trans*. **2015**, *44*, 4859−4873.

(17) Bozdag, M.; Ferraroni, M.; Nuti, E.; Vullo, D.; Rossello, A.; Carta, F.; Scozzafava, A.; Supuran, C. T. Combining the tail and the ring approaches for obtaining potent and isoform-selective carbonic anhydrase inhibitors: solution and X-ray crystallographic studies. *Bioorg. Med. Chem*. **2014**, *22*, 334−340.

(18) (a) Maresca, A.; Temperini, C.; Vu, H.; Pham, N. B.; Poulsen, S. A.; Scozzafava, A.; Quinn, R. J.; Supuran, C. T. Non-zinc mediated inhibition of carbonic anhydrases: coumarins are a new class of suicide inhibitors. *J. Am. Chem. Soc*. **2009**, *131*, 3057−3062. (b) Maresca, A.;Temperini, C.; Pochet, L.; Masereel, B.; Scozzafava, A.; Supuran, C. T. Deciphering the mechanism of carbonic anhydrase inhibition with coumarins and thiocoumarins. *J. Med. Chem*. **2010**, *53*, 335−344. (c) Ferraroni, M.; Carta, F.; Scozzafava, A.; Supuran, C. T. Thioxocoumarins show an alternative carbonic anhydrase inhibition mechanism compared to coumarins. *J. Med. Chem*. **2016**, *59*, 462-473. (d) Touisni, N.; Maresca, A.; McDonald, P. C.; Lou, Y.; Scozzafava, A.; Dedhar, S.; Winum, J.-Y.; Supuran, C. T. Glycosylcumarin carbonic anhydrase IX and XII inhibitors strongly attenuate the growth of primary breast tumors. *J. Med. Chem*. **2011**, *54*, 8271−8277. (e) Bonneau, A.; Maresca, A.; Winum, J. Y.; Supuran, C. T. Metronidazole-coumarin conjugates and 3-cyano-7-hydroxy-coumarin act as isoform-selective carbonic anhydrase inhibitors. *J. Enzyme Inhib. Med. Chem*. **2013**, *28*, 397−401. (f) Sharma, A.; Tiwari, M.; Supuran, C. T. Novel coumarins and benzocoumarins acting as isoform-selective inhibitors against the tumor-associated carbonic anhydrase IX. *J. Enzyme Inhib. Med. Chem*. **2014**, *29*, 292−296. (g) Tars, K.; Vullo, D.; Kazaks, A.; Leitans, J.; Lends, A.; Grandane, A.; Zalubovskis, R.; Scozzafava, A.; Supuran, C. T. Sulfocoumarins (1,2-benzoxathiine-2,2-dioxides): a class of potent and isoform-selective inhibitors of tumor-associated carbonic anhydrases. *J. Med. Chem*. **2013**, *56*, 293−300. (h) Tanc, M.; Carta, F.; Bozdag, M.; Scozzafava, A.; Supuran, C. T. 7-Substituted-sulfocoumarins are isoform-selective, potent carbonic anhydrase II inhibitors. *Bioorg. Med. Chem*. **2013**, *21*, 4502−4510.

(19) (a) Innocenti, A.; Vullo, D.; Scozzafava, A.; Supuran, C. T. Carbonic anhydrase inhibitors. Interactions of phenols with the 12 catalytically active mammalian isoforms (CA I−XIV). *Bioorg. Med. Chem. Lett*. **2008**, *18*, 1583−1587. (b) Innocenti, A.; Vullo, D.; Scozzafava, A.; Supuran, C. T. Carbonic anhydrase inhibitors. Inhibition of mammalian isoforms I−XIV with a series of substituted phenols including paracetamol and salicylic acid. *Bioorg. Med. Chem*. **2008**, *16*, 7424−7428.

(20) Carta, F.; Temperini, C.; Innocenti, A.; Scozzafava, A.; Kaila, K.; Supuran, C. T. Polyamines inhibit carbonic anhydrases by anchoring to the zinc-coordinated water molecule. *J. Med. Chem*. **2010**, *53*, 5511−5522.

(21) (a) Innocenti, A.; Scozzafava, A.; Supuran, C. T. Carbonic anhydrase inhibitors. Inhibition of cytosolic isoforms I, II, III, VII and XIII with less investigated inorganic anions. *Bioorg. Med. Chem. Lett.***2009**, *19*, 1855−1857. (b) Innocenti, A.; Scozzafava, A.; Supuran, C. T. Carbonic anhydrase inhibitors. Inhibition of transmembrane isoforms IX, XII and XIV with less investigated inorganic anions. *Bioorg. Med. Chem. Lett*. **2010**, *20*, 1548−1550.

(22) Temperini, C.; Scozzafava, A.; Supuran, C. T. Carbonic anhydrase inhibitors. X-Ray crystal studies of the carbonic anhydrase II-trithiocarbonate adduct. An inhibitor mimicking the sulfonamide and urea binding to the enzyme. *Bioorg. Med. Chem. Lett*. **2010**, *20*, 474−478.

(23) (a) Carta, F.; Aggarwal, M.; Maresca, A.; Scozzafava, A.; McKenna, R.; Supuran, C. T. Dithiocarbamates: a new class of carbonic anhydrase inhibitors. Crystallographic and kinetic investigations. *Chem. Commun*. **2012**, *48*, 1868−1870. (b) Avram, S.; Milac, A. L.; Carta, F.; Supuran, C. T. More effective dithiocarbamate derivatives inhibiting carbonic anhydrases, generated by QSAR and computational design. *J. Enzyme Inhib. Med. Chem*. **2013**, *28*, 350−359. (c) Carta, F.; Aggarwal, M.; Maresca, A.; Scozzafava, A.; McKenna, R.; Masini, E.; Supuran, C. T. Dithiocarbamates Strongly Inhibit Carbonic Anhydrases and Show Antiglaucoma Action in Vivo. *J. Med. Chem*. **2012**, *55*, 1721−1730.

(24) Carta, F.; Akdemir, A.; Scozzafava, A.; Masini, E.; Supuran, C. T. Xanthates and trithiocarbonates strongly inhibit carbonic anhydrases and show antiglaucoma effects in vivo. *J. Med. Chem*. **2013**, *56*, 4691−4700.

(25) Khalifah, R. G. The carbon dioxide hydration activity of carbonic anhydrase. I. Stop-flow kinetic studies on the native human isoenzymes B and C. *J. Biol. Chem*. **1971**, *246*, 2561−2573.

(26) Green D. L.; McCormick, B. J.; Pierpont, C. G. Amine adducts of thiocarbamate complexes. Crystal and molecular structure of bis(cyc1opentamethylenethiocarbamato)bis(piperidine)zinc(II). *Inorg. Chem.* **1973**, *12*, 2148−2151.

(27)Srivastava, D. K.; Jude, K. M.; Banerjee, A. L.; Haldar, M.; Manokaran, S.; Kooren, J.; Mallik, S.; Christianson, D. W. Structural analysis of charge discrimination in the binding of inhibitors to human carbonic anhydrases I and II. *J. Am. Chem. Soc.***2007**, *129*, 5528-5537.

(28) (a) Hans, M.; Wouters, J.; Demonceau, A.; Delaude, L. Synthesis and organocatalytic applications of imidazol(in)ium-2-thiocarboxylates. *Eur. J. Org. Chem.* **2011**, 7083–7091. (b) Ferm, R. J. The chemistry of carbonyl sulfide. *Chem. Rev.* **1957**, *57*, 621–640.

(29) Hawthorne, S. L.; Fay, R. C. Stereochemically rigid seven-coordinate complexes. Synthesis, structure, and dynamic stereochemistry of chlorotris(N,N-dialkylmonothiocarbamato)titanium(IV) complexes. *J. Am. Chem. Soc*. **1979**, *18*, 5268-5277.

(30) Zagidullin, R. N. Synthesis of dithio- and thiocarbamates of alkali and heavy metals based N-(β-aminoethyl)piperazine. *Khim.Geterotsikl*.,**1989**, *11*, 1524-1528.

(31) Bayly, C. I.;Cieplak, P.; Cornell, W. D.;Kollman, P.A. A well-behaved electrostatic potential based method using charge restraints for determining atom-centered charges: The RESP model. *J. Phys. Chem*. **1993**, *97*, 10269–10280.

(32) Wang, J.; Wang, W.; Kollman, P. A.; Case, D.A. Automatic atom type and bond type perception in molecular mechanical calculations. *J. Mol. Graph. Model*. **2006**, *25*, 247–260.

(33) (a) Friesner, R. A.; Banks, J. L.; Murphy, R. B.; Halgren, T. A.; Klicic, J. J.; Mainz, D. T.; Repasky, M. P.; Knoll, E. H.; Shaw, D. E.; Shelley, M.; Perry, J. K.; Francis, P.; Shenkin, P. S.

Glide: A New approach for rapid, accurate docking and scoring. 1. Method and assessment of docking accuracy. *J. Med. Chem.* **2004**, *47*, 1739–1749. (b) Halgren, T. A.; Murphy, R. B.; Friesner, R. A.; Beard, H. S.; Frye, L. L.; Pollard, W. T.; Banks, J. L. Glide: A New approach for rapid, accurate docking and scoring. 2. Enrichment factors in database screening. *J. Med. Chem*. **2004**, *47*, 1750–1759.

(34) (a) Jorgensen, W. L.; Tirado-Rives, J.; The OPLS potential functions for proteins, energy minimizations for crystals of cyclic peptides and crambin. *J. Am. Chem. Soc*., **1988**, *110*, 1657−1666. (b) Jorgensen, W. L.; Maxwell, D. S.; Tirado-Rives, J. Development and testing of the OPLS all-atom force field on conformational energetics and properties of organic liquids. *J. Am. Chem. Soc.* **1996**, *118*, 11225−11236.

TOC Graphic

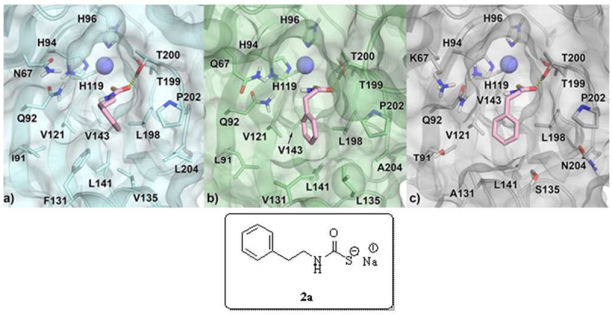
a)
H96
H94
N67
H119
T200
T199
P202
Q92
V121
V143
L198
I91
L204
L141
F131
V135
b)
H96
H94
Q67
H119
T200
T199
P202
Q92
V121
V143
L198
L91
A204
L141
V131
L135
c)
H96
H94
K67
H119
T200
T199
V143
P202
Q92
V121
L198
T91
N204
A131
L141
S135

2a